International Journal of High-Rise Buildings
December 2020, Vol 9, No 4, 369-376
https://doi.org/10.21022/IJHRB.2020.9.4.369

International Journal of
High-Rise Buildings
www.ctbuh-korea.org/ijhrb/index.php

Study on Integrity Assessment of Pile Foundation Based on Seismic Observation Records

Hisatoshi KASHIWA[1]

[1]*National Institute for Land and Infrastructure Management, Japan*

Abstract

Given the importance of quickly recovering livelihoods and economic activity after an earthquake, the seismic performance of the pile foundation is becoming more critical than before. In order to promote seismic retrofit of the pile foundations, it is necessary to develop a method for evaluating the seismic performance of the pile foundation based on the experimental data. In this paper, we focus on the building that was suffered severe damage to the pile foundation, conduct simulation analyses of the building, and report the results of evaluating the dynamic characteristics when piles are damaged using a system identification method. As a result, an analysis model that can accurately simulate the behavior of the damaged building during an earthquake was constructed, and it was shown that the system identification method could extract dynamic characteristics that may damage piles.

Keywords: soil-structure interaction, strong seismic records, damage of pile, simulation analysis, system identification

1. Introduction

Japan is one of the most earthquake-prone countries globally, and earthquake damage to buildings has been frequent since ancient times. On the other hand, due to repeated revisions of the standards for seismic design every time earthquake damage is experienced, the earthquake damage of superstructures built in accordance with the current standards is decreasing. While the superstructure has become harder to break due to an earthquake, damage to pile foundations tends to become apparent in recent earthquake damage. Although damage to pile foundations rarely directly leads to loss of life, it can have significantly impacted the re-occupancy of buildings after an earthquake. There are many cases where the building was demolished because the pile foundation was damaged, and the building was tilted, making it impossible to use the building. Given the importance of quickly recovering livelihoods and economic activity after an earthquake, it is essential to retrofit seismically to the pile foundation as needed. Seismic evaluation is required to carry out seismic retrofit, but it is difficult to investigate the pile foundation because that is underground, and a method for assessment of seismic performance for pile foundations has not been established.

Many studies on structural damage detection by indirect health monitoring have been carried out for a long time. In particular, there are several studies that use seismic observations to identify structural systems for dynamic soil-structure interaction problems, such as Safak (1995) or Stewart (1998), and pile damage detection is included in the system identification of dynamic soil-structure interaction problems. However, few cases are measured in buildings with damaged piles in actual seismic records, and there are not enough empirical research cases on pile damage detection.

In this paper, we focus on the building that was suffered severe damage to pile foundation, conduct simulation analyses of the building, and report the results of evaluating the dynamic characteristics when piles are damaged using a system identification method.

2. Outline of the 2016 Kumamoto earthquake and Target building

The target is a low-rise RC building that was damaged by the 2016 Kumamoto earthquake and has already been demolished.

The 2016 Kumamoto earthquake occurred mainly in Kumamoto Prefecture in Kyusyu district in Japan. The first shock, which is Mw 6.1 event, occurred on 14 April at 21:26 Japan Standard Time(JST) (GMT +9h). The mainshock, which is Mw 7.1 event, occurred on 16 April at 01:25 JST. Fig. 1 shows the location view of Kumamoto Prefecture and the epicenters of the first shock and mainshock. The twice large earthquakes destroyed over 7,000 wooden houses and residential buildings, mainly in the central area of Mashiki Town. Two seismic stations

†Corresponding author: Hisatoshi KASHIWA
Tel: +81-29-864-4270 , Fax: +81-29-864-6774
E-mail: kashiwa-h92ta@mlit.go.jp

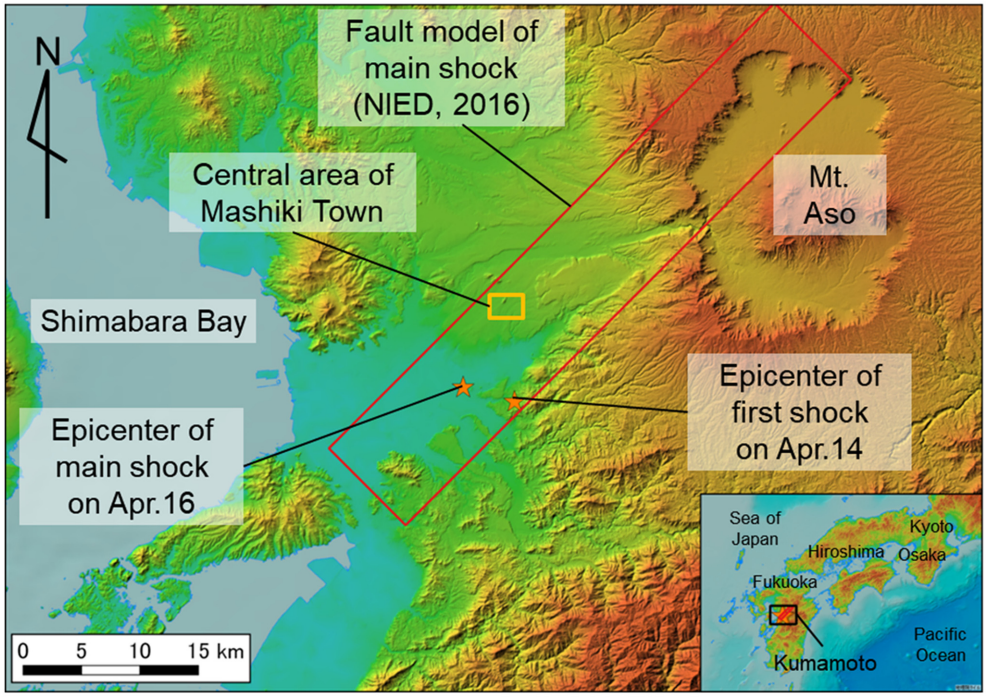


Figure 1. Location of Kumamoto Prefecture and the central area in Mashiki Town. (http://www.gsi.go.jp/LAW/2930-index.html, in Japanese.)

are in Mashiki Town. One is KiK-net KMMH16, operated by the National Research Institute for Earth Science and Disaster Prevention (NIED 2016) and was recorded seismic motion on the ground surface. Another is the Japan Meteorological Agency (JMA) seismic intensity station operated by a local government office (JMA 2016) and observed maximum value of seismic intensity, which is seven on twice seismic events. These seismic records are nearby the massive damage area of houses, as shown in Fig. 2.

JMA seismic intensity station was the records on the 1st floor in Mashiki Town Office, and these records were affected by the soil-structure interaction effects. Fig. 3 illustrates the Mashiki Town Office's general views, in

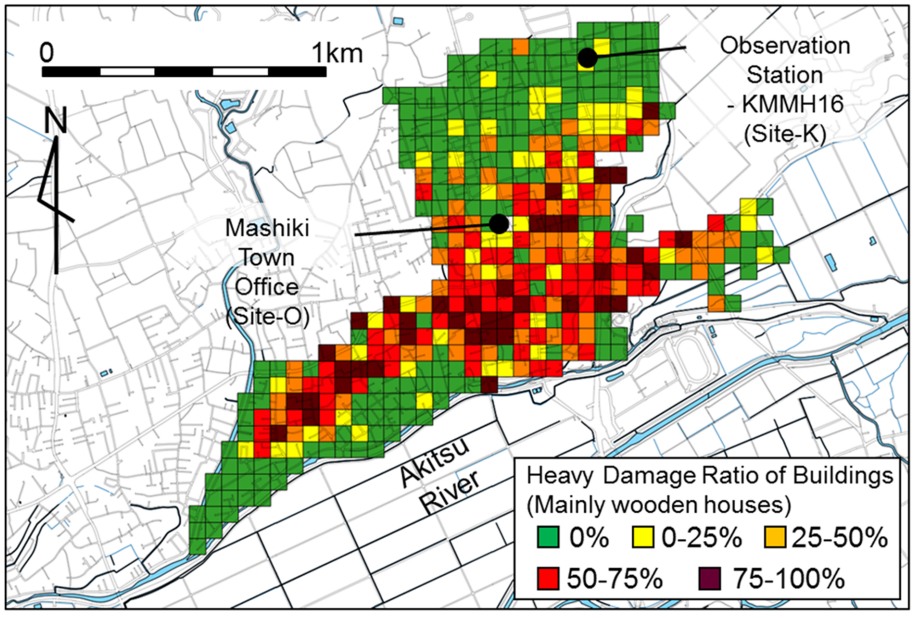


Figure 2. Location of observation stations, in which the spatial distribution of heavy damage ratio of wooden houses is illustrated. (NILIM 2016).

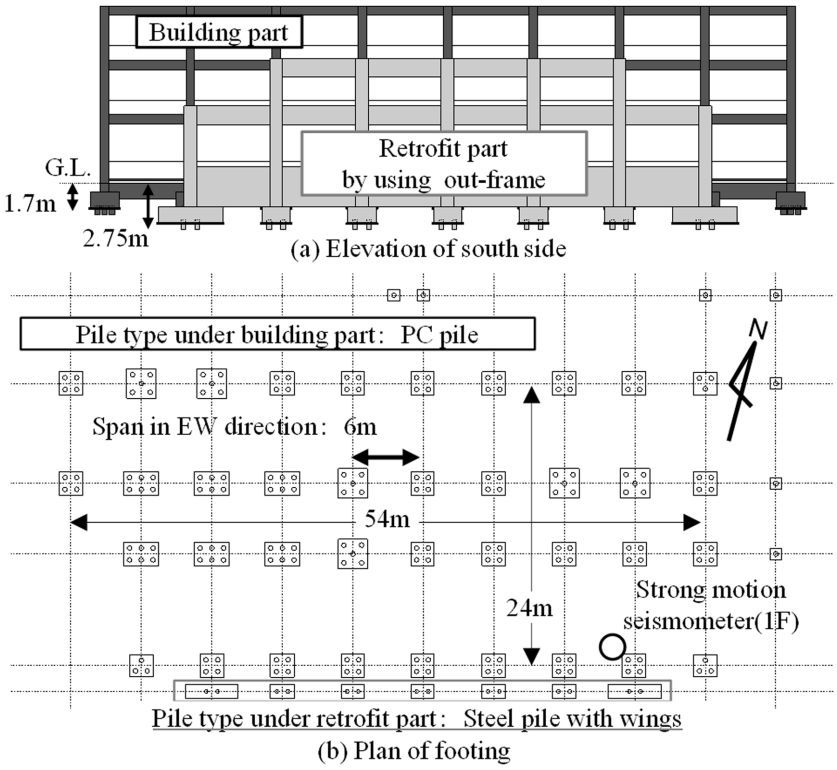


Figure 3. General views of Mashiki Town Office, in which the seismic records on the first floor observed during the first shock and mainshock.

which the seismic records on the 1st floor observed during the first and mainshock. This building is a three-story RC building supported by a pile foundation constructed in 1980 and retrofitted with out-flame to the south side in a longitudinal direction. The total number of piles is 192. The foundations under the existing part consist of isolated footings. Each footing is supported by one or 3~6 autoclave piles (AC pile), consisting of pile groups. The AC pile has 400 mm in diameter and 75 mm in thickness, and 26~32 m in length. The foundations under the retrofit part consist of isolated footings, each supported by two steel pipe piles with wings; the pile has 318.5 mm in diameter and 6.9mm in thickness, 27 m in length.

Fig. 4 shows the state of ground deformation around the building after the earthquakes. It can be seen that the gap between the building and the ground observed after the foreshock increased after the mainshock. Post-earthquake damage evaluation for the building was performed after the mainshock, and the damage grade of this building was moderate. Three corner piles were investigated by visual inspection and IT tests. Consequently, there were two massive damaged AC piles near the pile cap under the west side footing. The building's natural frequency is 3.0~4.0 Hz, where the value was measured using microtremor (Mori 2017).

Fig. 5 shows the borehole dates at two sites: Site-K and Site-O. In both Site-K and Site-O, the stratigraphy includes

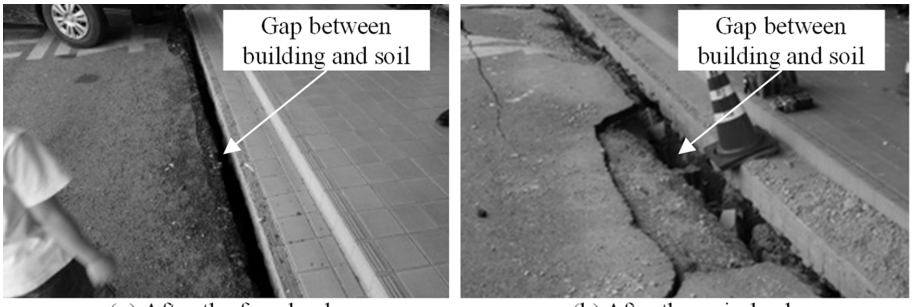


Figure 4. Gap between the building and the ground at east side of Mashiki town office after the earthquakes.

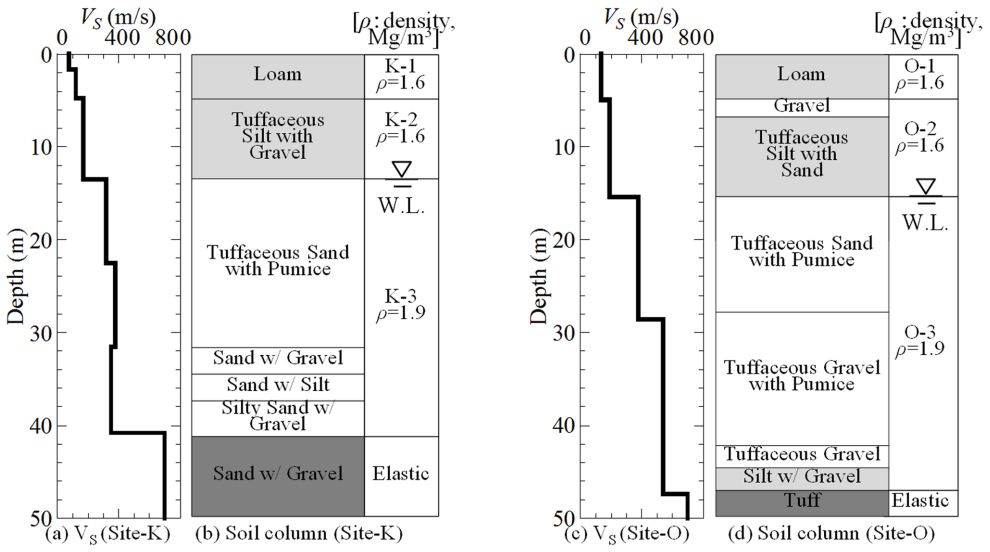


Figure 5. Soil classifications and S-wave(VS) velocity profiles for the analyses. (Kashiwa et al. 2019)

about 15 m of cohesive soil: loam, tuffaceous silt with gravel or sand, and tuffaceous sand with pumice or sandy soil at a depth from about 15 m to engineering bedrock, whose S-wave velocity is 700 m/s at a depth of about 40 m in this paper. Fig. 3(a) and (c) are S-wave velocity using in the simulation analysis. S-wave velocity at Site-K, as shown in Fig. 3(a), is determined by PS logging, and the S-wave velocity at Site-O, as shown in Fig. 3(c), is estimated by microtremor observation (Arai et al. 2017).

3. Simulation of seismic behavior of the building

Earthquake response analyses of dynamic soil-structure interaction are conducted at the Mashiki Town Office using the multi-lumped-mass beam spring model, as shown in Fig. 6. Here, from the plan in Fig. 3(b), the footing of the four piles is selected, the piles are replaced with a single pile, and the superstructure and pile are modeled into one beam spring model.

The superstructure is assumed to maintain linear behavior and has a rigid foundation. The reason for setting the superstructure as elastic is that the actual damage to the superstructure was small, and the actual yield strength is unknown. The weight of each floor of the superstructure is determined based on the design document. The first natural frequency of the superstructure is 4.0 Hz. The pile is modeled by beam element, and the model has nonlinearity considered a fiber section. The pile model has the same bending stiffness as the pile groups and is connected rigidity to the rigid foundation. The length of the pile model is 28 m. The S-wave velocity of soil

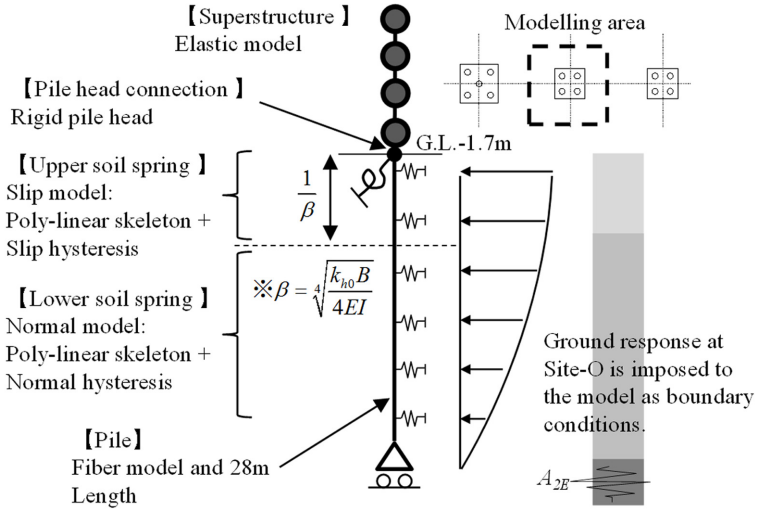


Figure 6. Schematic view of analytical model of Mashiki town office for earthquake response analysis considering soil-structure interaction effects

around the pile end is about 500 m/s. The pile model is supported on the side by interaction springs, which are Winkler-type springs, and at the end by pin-roller support. The pile group effect is assumed in the interaction spring's property. The interaction springs have a multi-linear backbone curve and a slip or Masing's hysteresis characteristic. The multi-linear backbone curves, which are consisted of five linear lines, are defined based on AIJ Recommendation (AIJ 2001). Slip hysteresis characteristic is only adopted up to the depth of $1/\beta$ (Railway Technical Research Institute 2012), and Masing's hysteresis characteristic is adapted to the other interaction springs. The time history of acceleration at bedrock (A^{2E}) is input to the entire model, and that of velocity and displacement of the seismic response of the free ground is input to the interaction springs. The bedrock motion and the velocity and displacement motion of the end of the interaction springs are estimated by inversion analysis at Site-K.

For details on other analysis settings, refer to Kashiwa et. al. (2019).

The acceleration time histories and pseudo velocity response spectra are shown in Fig. 7, which compare the observation and the calculation. Amplitudes and phases of the acceleration histories on the base foundation in the calculation, Cal(BF), are almost the same in the observation, Obs(BF), in both cases of the first shock and the mainshock. However, the spike shape in the acceleration history in Cal(BF) case is due principally to the hardening behavior of the interaction springs. The pseudo velocity response spectra of Cal(BF) are almost the same as that of Obs(BF). On the other hand, The pseudo velocity response spectra of Obs(BF) is smaller than that of Cal(GL) for the periods in the range of 0.2~0.6 s, whereas larger above 1.0 s. This indicates that when nonlinear behaviors, which are the local nonlinearity of the ground such as the gap or the structural nonlinearity such as the pile damage, occur, the response of the ground surface and the base foundation may differ significantly.

The maximum bending moment distributions of the pile and the maximum deformation distributions of the interaction springs during the first shock and the mainshock are shown in Fig. 8. My is the yield moment of the pile, Mu is the ultimate moment of pile, and yp is the threshold for whether there is a gap between the ground and the building. As shown in Fig. 8(b), the maximum bending moment at the pile cap on the first shock are close to the ultimate state. Moreover, as shown in Fig. 8(c), it can be seen that a large relative displacement occurs between the ground and the pile near the ground surface.

When the relative displacement between the pile and the ground is large near the ground surface, the inertial interaction effect is dominant. Therefore, using the superstructure specification as a parameter, analyses are conducted when the superstructure becomes a nonlinear state, and the influence of the inertial interaction effect is investigated. Fig. 9 shows the analysis results when the superstructure is considered with an inelastic state during the first shock. The story shear coefficient is 0.5. As shown in Fig. 9(b), the maximum story drift is significantly increased by allowing the superstructure to yield. Simultaneously, the bending moment of the pile is reduced, and it does not yield as shown in Fig. 9(c). At this time, the acceleration response on the base foundation

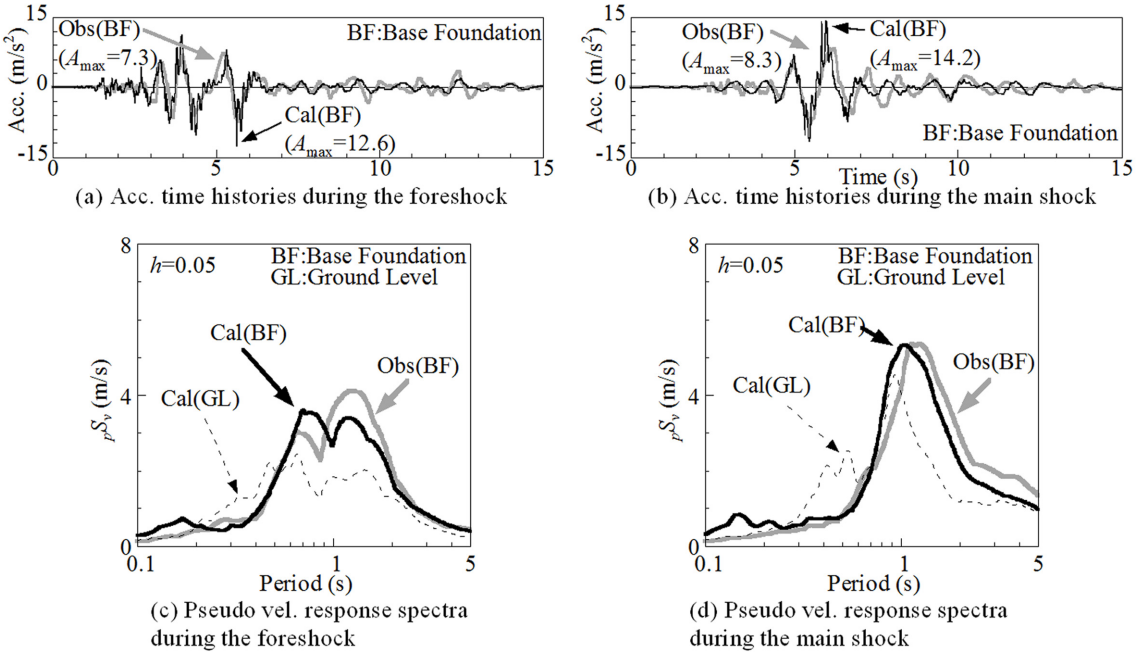


Figure 7. Comparisons between the calculation result(Cal) and the strong motion record(Obs) at Site-O and Mashiki Town Office.

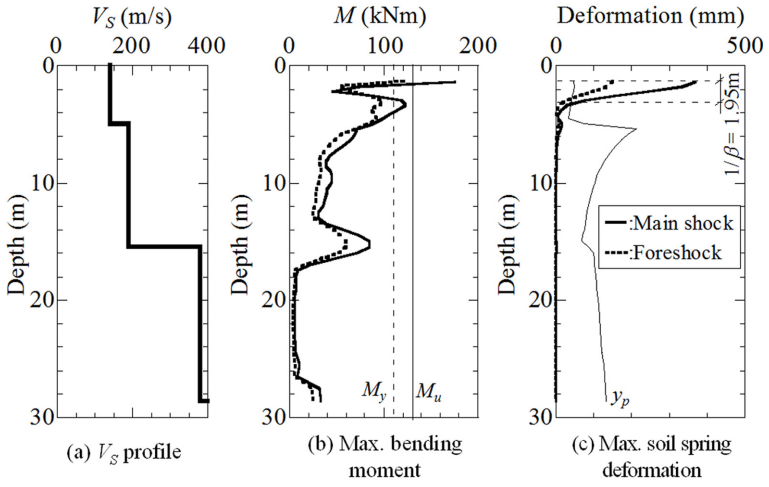


Figure 8. Max. response of bending moment and soil spring deformation.

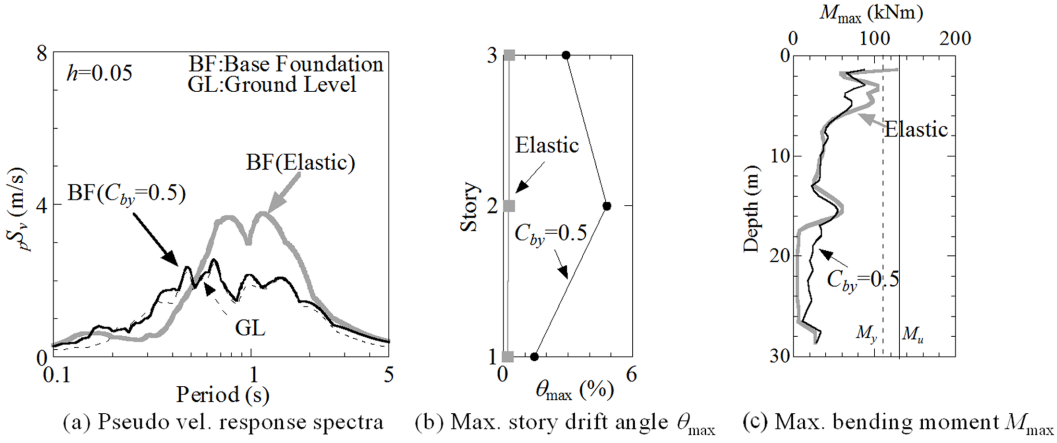


Figure 9. Analysis results during the first shock when superstructure is considered with inelastic state. (C_{by} = 0.5)

also changes significantly, and the pseudo velocity response spectrum of Cal(BF) is almost the same as that of GL.

4. Natural frequency evaluation by using Subspace identification

The system identification method is applied to the analysis results during the first shock shown in Chapter 3. The system identification method adopted in this paper is MOESP-type subspace model identification (Verhaegen 1992).

Fig. 10 shows the schematic view of the response of the superstructure considered with the dynamic soil-structure interaction. In this study, the ground surface (y_{ff}), the foundation (z_0), and the roof (z_1) responses are used for input and output motion in MOESP-type subspace model

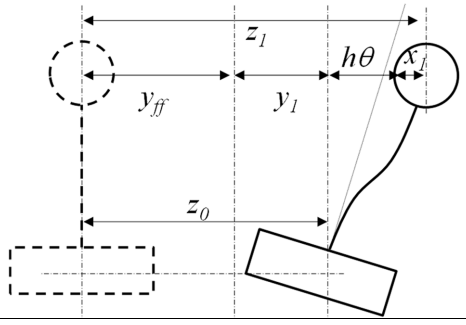


Figure 10. Schematic view of response.

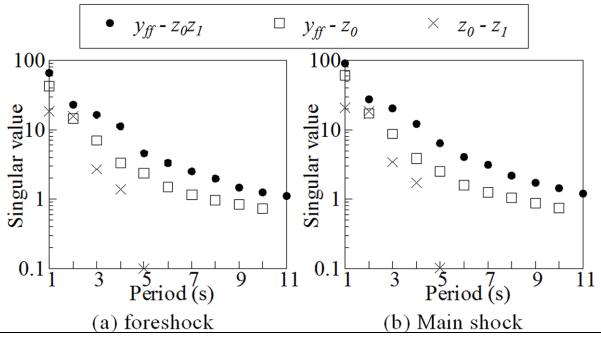


Figure 11. Singular value.

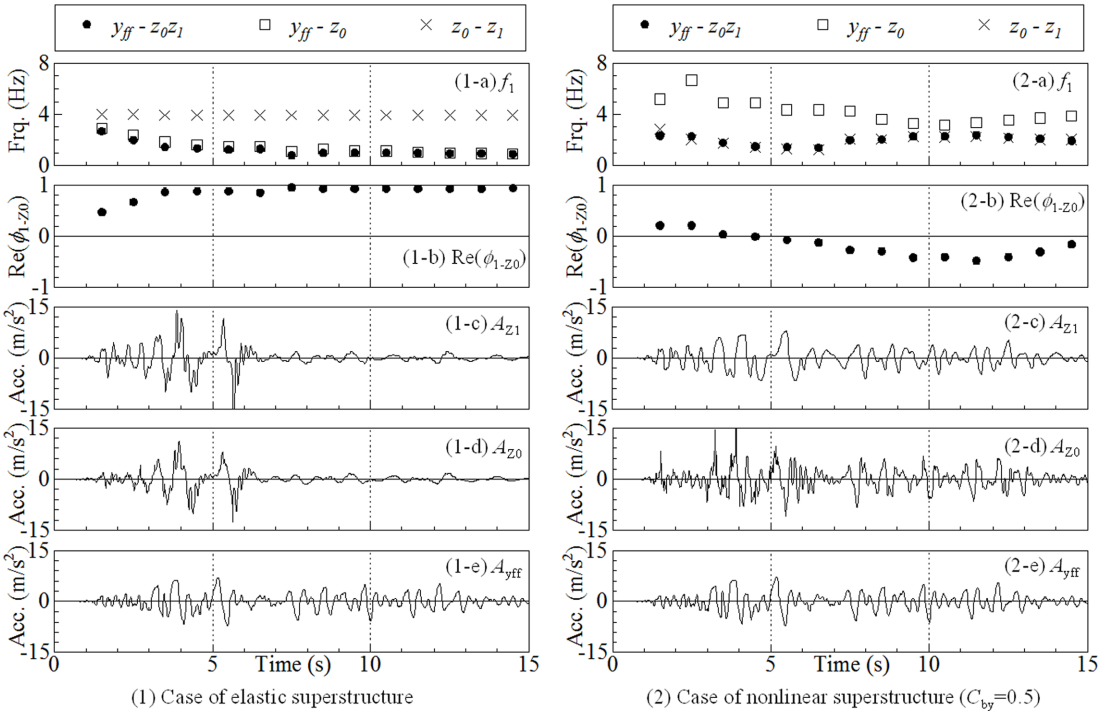


Figure 12. Analysis results of system identification.

identification. Three types of input and output combinations are considered. One is that the input is y_{ff}, and the outputs are z_0 and z_1, represented as y_{ff} - z_0z_1. The other is that the input is y_{ff}, and the output is z_0, represented as y_{ff} - z_0. which is the actual case of Mashiki Town Office. Another is that the input is z_0, and the output is z_1, represented as z_0 - z_1. which is focused on the dynamic characteristic of the superstructure in a base fixed condition. The sampling frequency of these responses is 100Hz. The data length of the block Hankel matrix is 301. The number of rows in the matrix is 10 in one output or 20 in two outputs. Fig. 11 shows the singular value per order for determining the number of orders to be identified. In this study, the number adapts 4.

Fig. 12 shows the analysis results of system identification, f_1 is 1st natural frequency, $f_{1\text{-}z0}$ is the value of z_0 in 1st mode normalized the value of z_1. The time histories of acceleration of z_1, z_0, and y_{ff} is also shown in Fig. 12. If the superstructure is kept elastic state, the 1st natural frequency of y_{ff} - z_0z_1 and y_{ff} - z_0 change almost the same with time, and z_0 - z_1 is constant at 4 Hz, initial 1st natural frequency of the superstructure. Furthermore, the real part of $f_{1\text{-}z0}$ is almost 1, which means the responses both z_0 and z_1 are almost the same, and the relative displacement between y_{ff} and z_0 is dominant. On the other hand, if the plasticity of the superstructure is allowed, the 1st natural frequency of y_{ff} - z_0z_1 and z_0 - z_1 change almost the same with time, which means the relative displacement between y_{ff} and z_0 is almost 0.

Therefore, in the case of Mashiki Town Office in the Kumamoto Earthquake, it is possible to roughly evaluate the characteristic of seismic behavior due to pile damage or superstructure damage by using the response acceleration of the ground surface, on the foundation, and on the roof, in which the significant relative displacement between the ground and the building occurs.

5. Conclusions

Simulation analyses of the RC building supported by piles subjected to very large seismic oscillation are conducted using a multi-lumped-mass beam spring model to evaluate the nonlinear soil-structure interaction effect seismic behavior of the superstructure and pile foundation. As a result, an analysis model that can accurately simulate the behavior of the damaged building during an earthquake was constructed. Furthermore, it was shown that the system identification method could extract dynamic characteristics that may damage piles. The development of a method for quantitatively extracting dynamic characteristics that lead to damage to piles under several building conditions and the ground properties is further study.

Acknowledgments

The authors would like to thank for the providing strong-motion records: K-NET and KiK-net operated by National Research Institute for Earth Science and Disaster Prevention (NIED), Japan Meteorological Agency (JMA),

and the local government office.

References

AIJ (2001). Recommendations for design of building foundations.

Arai, H. and Kashiwa, H. (2018). "Estimation of S-wave velocity profiles from microtremor and borehole surveys in damaged area during the 2016 Kumamoto Earthquakes, Japan." Proc. the 16th European Conference on Earthquake Engineering.

Japan Meteorological Agency, Japan (JMA) (2016). http://www.data.jma.go.jp/svd/eqev/data/kyoshin/jishin/1604142126_kumamoto/index2.html http://www.data.jma.go.jp/svd/eqev/data/kyoshin/jishin/1604160125_kumamoto/index2.html

Kashiwa, H., Arai, H. and Nakagawa, H. (2019). "Soil-structure interaction effects on strong motion records at Mashiki Town Office during the 2016 Kumamoto earthquakes" *Journal of Structural and Construction Engineering*, Vol.84, Issue 756, pp.183-193. (in Japanese with English abstract)

Kozo Keikaku Engineering Inc. (2017). RESP-F3T User's Manual. (in Japanese)

Mashiki Town Office (1979). Report on geological investigations for town office buildings. (in Japanese)

Mori, M. (2017). Damage situation and seismic response estimation of Mashiki City Hall under the 2016 Kumamoto Earthquake, Workshop about investigation for soil-structure interaction behavior and seismic design considered with SSI effects, AIJ: 41-48. (in Japanese)

National Institute for Land and Infrastructure Management, Japan (NILIM) (2016). Report of committee for causal analyses on damage to buildings during the 2016 Kumamoto earthquakes: 29-38. http://www.nilim.go.jp/lab/hbg/0930/report.htm (in Japanese)

National Research Institute for Earth Science and Disaster Resilience, Japan (NIED) (2016). http://www.kyoshin.bosai.go.jp/kyoshin/topics/Kumamoto_20160416/inversion_en/inv_public.htm http://www.kyoshin.bosai.go.jp/cgi-bin/kyoshin/db/sitedat.cgi?1+KMMH16+kik

Railway Technical Research Institute (2012). Design Standards for Railway Structures and Commentary (Foundation Structure). (in Japanese)

Safak, E. (1995). Detection and identification of soil-structure interaction in buildings from vibration recordings, *Journal of Structural Engineering*, Vol. 121, No.5, ASCE, pp.899-906.

Stewart, J.P. (1998). System identification for evaluating soil-structure interaction effects in buildings from strong motion records, *Earthquake Engineering and Structural Dynamics*, Vol.27, pp.869-885.

Verhaegen, M. and Dewilde, P. (1992). Subspace model identification Part1. The output-error state-space model identification class of algorithms, *Journal of Control*, Vol.56, No.5, pp.1187-1210